Dynamical mean-field study of model double-exchange superlattices

Chungwei Lin, Satoshi Okamoto, and Andrew J. Millis

Department of Physics, Columbia University, 538 West 120th Street, New York, New York 10027, USA

A theoretical study of [001] "double-exchange" superlattices is presented. The superlattice is defined in terms of an ABO_3 perovskite crystal. Itinerant electrons hop among the B sites according to a nearest-neighbor tight binding model and are coupled to classical "core spins." The A sites contain ionic charges arranged to form a [001] superlattice that forces a spatial variation of the mobile electron charge on the B sites. The double-exchange interaction is treated by the dynamical mean-field approximation, while the long-range Coulomb interaction is taken into account by the Hartree approximation. We find the crucial parameter is the Coulomb screening length. Different types of phases are distinguished and the interfaces between them classified.

"Strongly correlated" transition metal oxides are of great current interest because of the wide variety of the ordered phases they exhibit.[1] A particularly striking feature is the strong coupling between order and the ability of electrons to move through the crystal. For example, to the best of our knowledge the Goodenough-Karanori[2,3] rules establish a connection between orbital ordering and the overlap of electron wave functions between different sites, while in double-exchange systems such as the colossal magnetoresistance manganites, relative spin orientation strongly couples to hopping amplitudes.[4] Very recently, experimentalists have succeeded in fabricating high quality atomic-scale "digital heterostructures" consisting of combinations of correlated materials, typically characterized by different free carrier density and by different forms of long-range order. An example of a digital heterostructure is [001] $(LaMnO_3)_m(SrMnO_3)_n$:[5–8] m planes of $LaMnO_3$ followed by n planes of $SrMnO_3$, with the whole making a periodic structure with a repeat distance of $m+n$ times the mean Mn-Mn c-axis distance. Here $LaMnO_3$ (one electron per Mn e_g state) and $SrMnO_3$ (no electrons per Mn e_g state) are the two end-member compounds of the "colossal magnetoresistance" (CMR) alloy $La_{1-x}Sr_xMnO_3$ family of compounds.

This experimental success raises fundamental questions. Correlated electron materials are interesting because of the phases they exhibit (for example, magnetic, superconducting, and Mott insulating). In correlated electron heterostructures, the key questions are: What phases can occur, and what is the spatial structure; in particular, what is the character of the domain walls which separate regions of different spatial orders? In this paper we present a detailed study of a simple model which yields insight into these issues.

Our model is motivated by the colossal magnetoresistance heterostructures now being fabricated.[5–8] It involves a heterostructure defined electrostatically by a periodic array of charged counter ions,[9,10] with carriers subject to the double-exchange (DE) interaction[11,12] which is crucial to the physics of the CMR materials. The lattice structure considered here is based on the ABO_3 perovskite structure with lattice constant a, and we shall be interested in structures of the form $(ABO_3)_m(A'BO_3)_n$ [(m,n) heterostructure] periodic in the [001] direction. A schematic representation is shown in Fig. 1 for the (2,1) heterostructure. A and A' have ion charge +1 and 0 (neutral) relative to B site, and therefore the total electron density per unit cell is $m/(m+n)$. We place the electrically active B sites in planes $z=pa$ with p an integer, m charge +1 ions in planes $z=(p+\frac{1}{2})a$ with $p=1$ to m, and n charge 0 ions in planes $z=(p'+\frac{1}{2}+m)a$ with $p'=1,\dots,n$. The conduction electron hopping between B sites is described by a one orbital tight binding model.

The Hamiltonian is

$$H_{tot} = H_{hop} + H_{Hund} + H_{Coul}, \qquad (1)$$

with

$$H_{hop} = -t \sum_{\langle i,j \rangle, \sigma} (c_{i,\sigma}^{\dagger} c_{j,\sigma} + \text{H.c.}), \qquad (2)$$

$$H_{Hund} = -J \sum_i \vec{S}_i \cdot \vec{\sigma}_{\alpha,\beta} c_{i,\alpha}^{\dagger} c_{i,\beta}, \qquad (3)$$

and

$$H_{Coul} = \sum_{i \neq j} \left[\frac{1}{2\varepsilon} \frac{e^2 n_i n_j}{|\vec{r}_i - \vec{r}_j|} + \frac{1}{2\varepsilon} \frac{e^2}{|\vec{R}_i^A - \vec{R}_j^A|} - \frac{e^2 n_i}{\varepsilon |\vec{r}_i - \vec{R}_j^A|} \right], \quad (4)$$

with $n_i = \Sigma_\sigma c_{i,\sigma}^{\dagger} c_{i,\sigma}$ the occupation number at B site $\vec{r}_i \cdot \vec{r}_i$ and $\vec{R}_i^A$ label the positions of the B and A sites, respectively, and ε is the dielectric constant of the material. To solve this model, we use the dynamical mean-field theory[10,13,14] for the double-exchange interaction and Hartree approximation for the long-range Coulomb interaction. Because the core spin is classical, we solve the impurity model by direct evaluation of the partition function. The leading instability of the paramagnetic phase is obtained using the method of Ref. 15, the FM-PS (where FM denotes ferromagnetic and PS phase separation) phase boundary and also the $T=0$ phase boundaries are obtained by the methods developed in Refs. 13 and 16 while the FM-AF (AF is antiferromagnetic) phase boundary is estimated by computing the energy and entropy difference between different phases. Details of the calculations will be presented elsewhere.
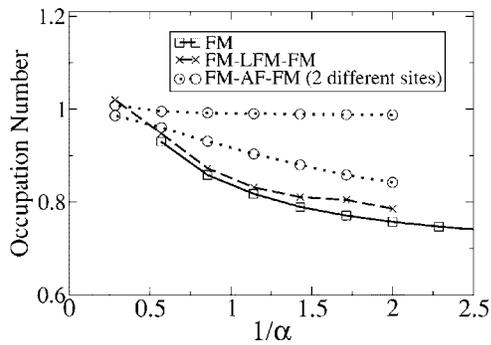
FIG. 1. Schematic representation of a $(ABO_3)_2(A'BO_3)_1$ (2,1) superlattice. Counterions A and A', located at positions $z=(p+\frac{1}{2})a$ (with p an integer), are represented by their relative charges +1 and 0, respectively, whereas the two symmetry-different B sites, located at integer positions, are represented by filled and open circles.

In this model, the heterostructure is defined by Coulomb forces, the important order is magnetic, and the coupling between order and itinerancy is via the double-exchange mechanism. However, we expect our qualitative conclusions to apply more generally to any situation in which the charge density varies across the heterostructure and the physics involving a coupling between order and charge mobility.

The model we study involves two fundamental parameters: $\alpha=e^2/\varepsilon ta$, measuring the strength of the Coulomb interaction relative to the electron hopping, and the Hunds coupling J/t, expressing the magnitude of on-site spin polarization and thus the degree to which magnetic order controls electron hopping. Our results are not very sensitive to the magnitude of J/t, provided it is large enough that the conduction band is fully polarized in FM ground state, so we take $J/t=6$, a value believed to be roughly consistent with the values found in the CMR materials.

The important parameter is α. It is sometimes convenient to express α in terms of a screening length $L_{TF}\approx a/\alpha$. At small α, the charge is only weakly confined, so for short period structures, the charge is uniformly distributed and the system exhibits essentially the same phase as is found in the randomly doped bulk material. For long period heterostructures, there is a gradual charge modulation from $n\approx 1$ (ABO_3) to $n\approx 0$ ($A'BO_3$). In this latter case, the known bulk phase diagram[16,17] leads us to expect a spatial variation of the magnetic phases, from the AF in the $n\approx 1$ region, to PS in the intermediate transition region, and to ferromagnetic in the lower density $A'BO_3$ region. For large α, the charge profile is more abrupt, and the possibility of a sharp AF and/or FM domain wall exists. To study this case in more detail we consider a (2,1) heterostructure which is simple enough to study in detail and will be seen to capture a wide range of phenomena.

The (2,1) heterostructure has two electronic regions: a bilayer of B sites, denoted by open circles in Fig. 1, each with one A (with charge+1) and A' (with charge 0) site as neighbor, and, therefore, a relatively lower charge density; and a single layer of B sites (denoted by shaded circles in Fig. 1) with two A sites as neighbors and therefore a relatively higher charge density. The behavior of bilayers is found to be simple, being paramagnetic or ferromagnetic ac-

FIG. 2. (Color online) Phase diagram at a $T-1/\alpha$ plane for $J/t=6$, (2,1) superlattice. PM, paramagnet; LFM, layer ferromagnet; FM, ferromagnet; AF, antiferromagnet; PS, phase separation.

cording to the temperature. The behavior of the monolayer sandwiched by two A layers is more complicated, involving also an interplay between charge binding and the nature of the magnetic order. Figure 2 shows the calculated phase diagram in the temperature-charge binding interaction plane, with different phases labeled by the central layer spin correlations. The solid line marked by open circles indicates the Curie temperature, below which the outer layers order ferromagnetically. Near T_c the inner layer is ferromagnetic and is either aligned ($1/\alpha>0.6$) or antialigned ($1/\alpha<0.6$) to the outer layers (canted phases are not found). In either case the inner layer polarization is much smaller than that on the outer layer. When the Coulomb interaction is weak ($1/\alpha>3$), the charge density is weakly modulated relative to the mean value $\frac{2}{3}$ and ferromagnetism is observed at all $T<T_c$, consistent with the bulk phase diagram.[16,17]

As the charge binding is increased, the central layer charge density increases, eventually reaching values for which ferromagnetism is not favored in the bulk phase diagram. In this $1.4<1/\alpha<2.8$ region, at low T the central layer exhibits phase separation between ferromagnetic and antiferromagnetic states. Phase separation is also found in the bulk case in approximately this region, but the phase boundaries are slightly shifted because of a proximity effect arising from the FM outer layers. The FM-PS phase boundaries are found to be second order in this model.

As the charge binding is further increased, a temperature-driven first order FM and/or AF transition occurs. In this $0.6<1/\alpha<1.4$ region, the central layer charge densities correspond to values at which the corresponding bulk materials are phase separated between FM and AF states. We interpret this FM-AF-FM phase in the superlattice as a phase separation in the z direction: the relatively stronger charge binding means that it is energetically favorable for the system to phase separately by moving the charge only in the z direction. Finally, as the charge binding is yet further increased ($1/\alpha>0.6$), we find a new layer ferromagnet (LFM) phase where both central and outer layers are in-plane ferromagnetic but with magnetizations antialigned. This phase is not found in bulk calculation of the single-band DE model.

The transitions to the AF and LFM phases are first order, and are driven by the interplay of ordering and charge mo-

FIG. 3. α dependence of the central-layer charge density for different ordered phases at $T=0$. For the FM-AF-FM state, two values for two inequivalent sites are shown.

bility. Figure 3 shows the central layer charge density as a function of charge binding parameter, for the different homogeneous phases (the total charge density is, of course, fixed by charge neutrality). The plot displays the occupation number in the α regions where the phases are locally stable, whether or not a given phase is the ground state. The FM phase is most favorable for electronic itineracy, and therefore has the lowest central layer charge density and least favorable Coulomb energy. The AF phase has noticeably higher mean charge density, which moreover exhibits the expected sublattice structure, being highest on the sublattice with spin antiparallel to the ferromagnetic region because for this relative spin alignment, hopping is suppressed. At intermediate α the LFM phase has a lower charge density than the AF phase, essentially because the FM core spin arrangement results in a wider in-plane bandwidth than the AF and therefore forces more states (than AF) to be above the chemical potential. However, at sufficiently strong charge binding the central-layer occupation becomes larger than that of the AF state, so the LFM phase becomes favored by the Coulomb energetics.

We next discuss another general implication of our results. Figure 3 shows that the electronic density distribution is strongly affected by the magnetic order changing both with dielectric constant and with temperature. In the present model, this behavior is a consequence of the "double-exchange" physics of coupling of hopping amplitude to intersite spin correlations, but similar physics may also be expected to occur in orbitally degenerate systems, where hopping amplitudes depend on orbital overlaps which are changed by orbital order. This raises the intriguing possibilities of magnetoelectric coupling; for example, changing a charge density by applying a magnetic field large enough to eliminate the antiferromagnetism or changing magnetic behavior by "gating" the electron density.[18]

We now consider the implications of our results for more general heterostructures. A given system may be characterized by a charge screening length L_{TF}, which depends on both the charge screening parameter α and the nature of magnetic order (if any). Systems with $L_{TF}>(na,ma)$ exhibit bulklike behavior with average charge density $m/(m+n)$; systems with smaller L_{TF} may exhibit spatially differentiated behavior, with high density and low density regimes characterized by different kinds of long-ranged order. This is seen in the phase diagram shown in Fig. 2, where as L_{TF} is re-
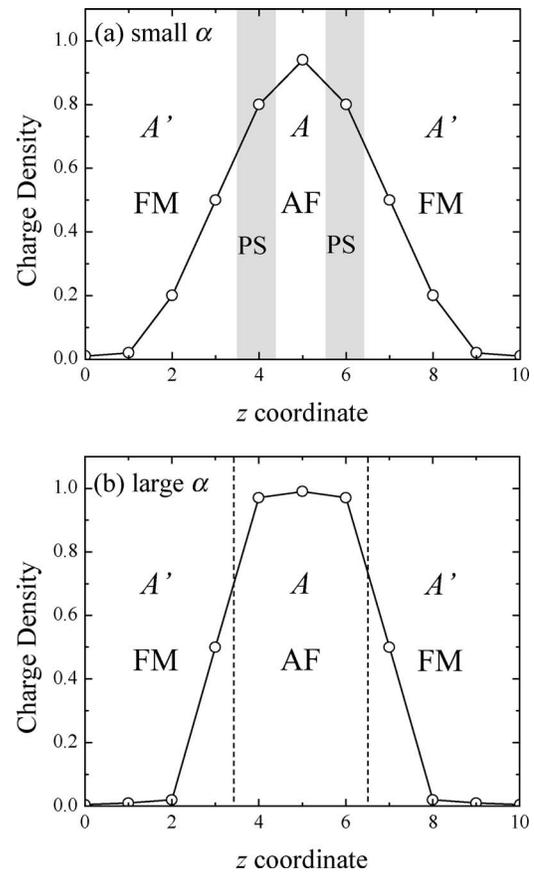

FIG. 4. Schematic representation of the expected electronic density and low T phase behavior of a long period $[m=4,n=6$ heterostructure, with A (charge+1) ions at positions $z=3.5,4.5,5.5,6.5]$. The central region is expected to exhibit order characteristics of the $n=1$ bulk material (Néel AF in the present case); the outer region is ferromagnetic, and the two regions are separated by a window of phase separation whose existence depends on the charge binding parameter α. (a) For weak charge binding (small α), there exists phase separated regions between FM and AF states; (b) for strong charge binding (large α), no intermediate state separates FM and AF states.

duced to below a value of the order of one lattice constant, the central layer exhibits a different form of long-ranged order than the outer layers. We expect the same behavior to occur in longer-period structures, with the obvious shifts in phase boundaries following from the changes in the length scales to which L_{TF} should be compared. The resulting two phase structures raises the issue of the interface between different phases. If L_{TF} is of order one lattice constant or less, then we expect an abrupt change of behavior, as is seen in the $1/\alpha \approx 1$ regime of Fig. 2, where one layer is AF and the adjacent layers are FM. However, if L_{TF} is larger [but still smaller than (ma,na)] then we expect a more gradual interface, with one or a sequence of intermediate phases. This behavior is seen in the "PS" range $(1.5<1/\alpha<2.9)$ of Fig. 2. Figure 4 depicts our expectation of the electronic density and the associated phase at each layer for a long period superlattice. AF and FM phases are separated by a phase separated region whose existence depends on the screening parameter α. We emphasize that these considerations should

apply not only to the specific double-exchange model considered here, but also to other situations in which long-ranged order is controlled by charge density, for example, those involving orbital ordering.

In conclusion, we have used a detailed analysis of a model system to gain insight into the electronic phase behavior of correlated electrons in electrostatically defined heterostructures. We have shown that the crucial parameter is the strength with electrons are bound to the high-density regions, and have distinguished the different types of phases which may occur and classified the types of interfaces between phases. Our findings also raise the possibility of an interesting magnetoelectric coupling. Important directions for future work include applying the ideas introduced here to orbital ordering, and going beyond model systems to make predictions for experimental systems.

[1] M. Imada, A. Fujimori, and Y. Tokura, Rev. Mod. Phys. **70**, 1039 (1998).

[2] J. B. Goodenough, *Magnetism and Chemical Bond* (Interscience Publishing, New York, 1963).

[3] J. Kanamori, J. Phys. Chem. Solids **10**, 87 (1959).

[4] C. Zener, Phys. Rev. **82**, 403 (1951).

[5] H. Tanaka, J. Zhang, and T. Kawai, Phys. Rev. Lett. **88**, 027204 (2002).

[6] J. Eckstein (private communication).

[7] M. Ohtomo, D. A. B. Muller, D. Grezul, and H. Y. Hwang, Nature (London) **419**, 378 (2002).

[8] H. Yamada, M. Kawasaki, Y. Ogawa, and Y. Tokura, Appl. Phys. Lett. **81**, 4793 (2002).

[9] S. Okamoto and A. J. Millis, Nature (London) **428**, 630 (2004); Phys. Rev. B **70**, 075101 (2004).

[10] S. Okamoto and A. J. Millis, Phys. Rev. B **70**, 241104(R) (2004).

[11] N. Furukawa, J. Phys. Soc. Jpn. **64**, 2734 (1995).

[12] A. J. Millis, R. Mueller, and B. I. Shraiman, Phys. Rev. B **54**, 5389 (1996); **54**, 5405 (1996).

[13] A. Georges, G. Kotliar, W. Krauth, and M. Rozenberg, Rev. Mod. Phys. **68**, 13 (1996).

[14] M. Potthoff and W. Nolting, Phys. Rev. B **60**, 7834 (1999).

[15] B. Michaelis and A. J. Millis, Phys. Rev. B **68**, 115111 (2003).

[16] C. W. Lin and A. J. Millis, Phys. Rev. B **72**, 245112 (2005).

[17] S. Yunoki, J. Hu, A. L. Malvezzi, A. Moreo, N. Furukawa, and E. Dagotto, Phys. Rev. Lett. **80**, 845 (1998).

[18] N. Nakakawa, M. Asai, Y. Mukunoki, and H. Y. Hwang, Appl. Phys. Lett. **86**, 082504 (2005).